Non-linear Speed Control of Elastic Systems with Backlash

Mattias Nordin[1] Per-Olof Gutman[2]

Abstract

Backlash in elastic systems is one of the most important non-linearities that limits the performance of speed control in industrial drives. In this work a new robust non-linear speed controller for such system is proposed. Two linear controllers are designed, one globally stable with reduced performance, and one with high performance exhibiting limit cycles around the backlash. The two controllers are combined into one high performance, stable non-linear controller with soft switching. The advantage of the new controller is shown with simulations and measurements on a large real life drive system.

1 Introduction

Many industrial drive systems can reasonably well be modeled as a two-mass system with backlash, see figure 1, together with the non-minimum phase dynamics of the actuator.

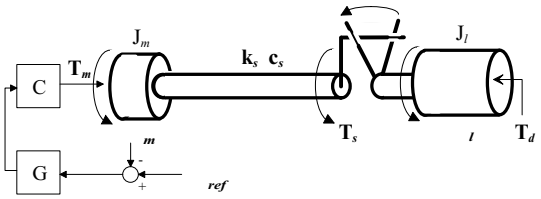

Figure 1: Feedback from motor speed. C denotes the actuator dynamics, and G the feedback control.

In this paper we study the motor speed regulation problem for two-mass systems with backlash, subject to torque disturbances on the driven load. Robust linear and non-linear controllers are designed, that minimize the *impact drop*, defined as the maximum integrated speed error of the system, subject to a load torque step.

[1] Metals and Mining Division, ABB Automation Systems AB, 721 67 Västerås, Sweden, mattias.c.nordin@se.abb.com

[2] Faculty of Agricultural Engineering, Technion — Israel Institute of Technology, Haifa 32000, Israel. peo@tx.technion.ac.il

2 A Model of a Two-mass System with Backlash

A two-mass system with backlash, as shown in figure 1 can be modeled as

$$\left\{ \begin{array}{rcl} J_m\dot{\omega}_m &=& -c_m\omega_m - T_s + T_m \\ J_l\dot{\omega}_l &=& -c_l\omega_l + T_s - T_d \\ \omega_d &=& \omega_m - \omega_l \end{array} \right. \quad (1)$$

with

$$T_s = k_s\theta_s + c_s\omega_s \quad (2)$$

$$\dot{\theta_m} = \omega_m, \quad \dot{\theta}_l = \omega_l, \quad \dot{\theta}_d = \omega_d,$$

and where J_m [kgm^2] is the motor moment of inertia, c_m [Nm/(rad/s)] is the viscous motor friction, T_s [Nm] is the transmitted shaft torque, T_m [Nm] is the motor torque, J_l [kgm^2] is the load moment of inertia, c_l [Nm/(rad/s)] is the viscous motor friction, T_d [Nm] is the load torque disturbance, k_s [Nm/rad] is the shaft elasticity, and c_s [Nm/(rad/s)] is the inner damping coefficient of the shaft. The angles θ_m, θ_l, $\theta_d = \theta_m - \theta_l$ are the motor angle, load angle, and difference angle [rad], respectively, while ω_m, ω_l, $\omega_d = \omega_m - \omega_l$ are their respective time derivatives; the motor angular velocity the load angular velocity, and the difference angular velocity [rad/s].

The backlash can be described by how the shaft twist angle θ_s depends on the motor and load speeds and angles ω_m, ω_l, θ_m, θ_l respectively. In [5, 6] a thorough analysis is presented. In this paper we will use the linear model without backlash, P_{linear} for which $\theta_s = \theta_d$, or the describing function of the exact model P_{exact}, with

$$\theta_s = \theta_d - \theta_b \quad (3)$$

where θ_b, representing the backlash angle, follows the non-linear dynamic equation

$$\dot{\theta}_b =$$

$$\left\{ \begin{array}{lll} \max(0, \dot{\theta_d} + \frac{k_s}{c_s}(\theta_d - \theta_b)) & \text{if} \quad \theta_b = -\alpha & (T_s \le 0) \\ \dot{\theta_d} + \frac{k_s}{c_s}(\theta_d - \theta_b) & \text{if} \quad |\theta_b| < \alpha & (T_s = 0) \\ \min(0, \dot{\theta_d} + \frac{k_s}{c_s}(\theta_d - \theta_b)) & \text{if} \quad \theta_b = \alpha & (T_s \ge 0) \end{array} \right. \quad (4)$$

where α [rad] equals the backlash gap. For full realism, the non-minimum phase actuator dynamics of the electrical drive system from motor torque reference T_r to motor torque T_m is assumed to be:

$$T_m(s) = \frac{e^{-s\tau_d}}{(1 + s\tau_e)} T_r \quad (5)$$

The designs in the paper will use the numerical values

$$\begin{cases} J_m & = & 0.4 & \text{kgm}^2 \\ c_m & \in & [0, 0.1] & \text{Nm/(rad/s)} \\ J_l & \in & [5.5, 6.0] & \text{kgm}^2 \\ c_l & \in & [0, 1] & \text{Nm/(rad/s)} \\ k_s & \in & [3000, 4000] & \text{Nm/rad} \\ c_s & \in & [1, 20] & \text{Nm/(rad/s)} \\ \tau_d & = & 0.006 & \text{s} \\ \tau_e & = & 0.008 & \text{s} \\ \alpha & = & 0.05 & \text{rad} \end{cases} \quad (6)$$

The nominal case is defined by the parameter combination $c_m = 0.1$, $J_l = 5.6$, $c_l = 1$, $k_s = 3300$, and $c_s = 1$.

3 Linear Design for the Plant without Backlash

It can be shown, see e.g. [6], that the plant with the backlash gap closed, e.g. due to a sufficiently large load torque T_d, behaves similarly to a linear plant without backlash. Without backlash, the design problem is reduced to a linear elastic SISO system with parametric uncertainty for which QFT achieves good design results [3]. From (1),(2) and $\theta_s = \theta_d$ (see P_{linear} above) we obtain the parameter dependent transfer function $P_l(s, q)$ from motor torque reference T_r to motor speed ω_m:

$$P_l = \frac{e^{-s\tau_d}}{(1 + s\tau_e)} \times \frac{J_l s^2 + (c_l + c_s)s + k_s}{d(s)} \quad (7)$$

where

$$d(s) = J_m J_l s^3 + (J_l(c_m + c_s) + J_m(c_m + c_s))s^2 +$$
$$+((J_l + J_m)k_s + c_m c_l + c_m c_s + c_l c_s)s + (c_m + c_l)k_s$$

and $q = (J_m, c_m, J_l, c_l, k_s, c_s, \tau_d, \tau_e)$ is the parameter vector with $q \in Q$ with Q defined by (6). In QFT, the plant uncertainty is represented by frequency dependent *templates* or value sets, $V(\omega) = \{P(j\omega, q)\} \forall q \in Q$. The templates are shown in figure 2.

The closed loop specifications are as follows: 1) Global stability; 2) Minimal impact drop which is approximately equivalent to maximizing the open loop low frequency gain 3) Shaft torque overshoot <80% for load torque steps; and 4) Sensitivity modulus < 6 dB. In QFT, frequency dependent, complex valued *Horowitz bounds* are calculated. For each frequency and specification the Horowitz bound is a constraint such that if the compensated nominal open loop satisfies it, then the specification is fulfilled for all plant cases.

PI-controller G_{PI} . We first design a PI controller in order to have a standard industrial design to compare our other designs with. Manual loop shaping gives the PI-compensator

$$G_{\text{PI}} = k_p \left(\frac{sT_i + 1}{sT_i} \right), \quad \begin{cases} k_p = 26 \\ T_i = 0.2 \end{cases} \quad (8)$$

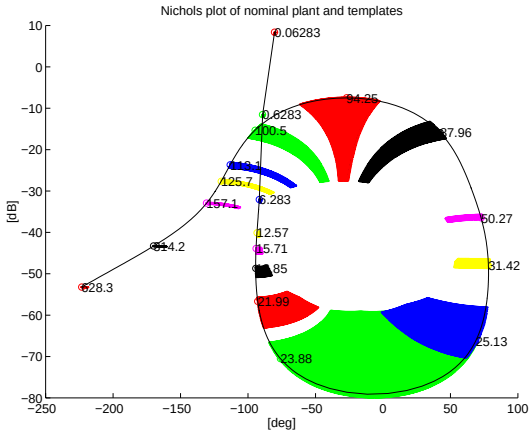

Figure 2: Templates, parameterized by frequency [rad/s] of the transfer function P_l in a Nichols chart. The rings denote the nominal plant case.

that makes the nominal compensated open loop satisfy the Horowitz bounds. With $T_i = \infty$ initially, k_p was tuned first by increasing its value as long as the sensitivity specifications was satisfied for high frequencies. Then T_i was reduced as much as possible, while still fulfilling the specifications. Thus k_p/T_i was maximized, and hence the impact drop is minimized. An analysis of the design [6] reveals that the limiting factor is the sensitivity specification. Step response simulations [6] show that the biggest torque overshoot is 55%, way below the specification, and the biggest impact drop on the load side is 2.5 rad.

High Gain Controller G_{high} . To achieve a better result more design freedom is needed. That is obtained by adding two complex links, i.e. using the controller structure

$$G(g) = k_p \left(\frac{sT_i + 1}{sT_i} \right) \times$$
$$\times \left(\frac{s^2/\omega_1^2 + 2\zeta_1/\omega_1 + 1}{s^2/\omega_2^2 + 2\zeta_2/\omega_2 + 1} \right) \times \left(\frac{s^2/\omega_3^2 + 2\zeta_1/\omega_3 + 1}{s^2/\omega_4^2 + 2\zeta_4/\omega_4 + 1} \right) \quad (9)$$

where

$$g = \{k_p, T_i, \omega_1, \zeta_1, \omega_2, \zeta_2, \omega_3, \zeta_3, \omega_4, \zeta_4\}$$

defines the controller parameters. The first link is used as a complex lag link for the frequency interval between the resonance and anti-resononce. The second link is then used as a complex lead link for the second cross-over frequency. It is then possible to raise k_p/T_i from $26/0.09 \approx 289$ to $160/0.09 \approx 1780$. The final design is chosen to be $G_{\text{high}} \stackrel{\text{def}}{=} G(g_{\text{high}})$ with $g_{\text{high}} = \{k_p = 160; T_i = 0.2; \omega_1 = 80; \zeta_1 = 0.25; \omega_2 = 80; \zeta_2 = 0.55; \omega_3 = 85; \zeta_3 = 0.2; \omega_4 = 45; \zeta_4 = 0.25\}$. In figure 3 the compensated nominal open loop is shown together with some of the critical bounds.

The step response torque overshoots are found, see [6], to be much higher for this design than for the PI design.

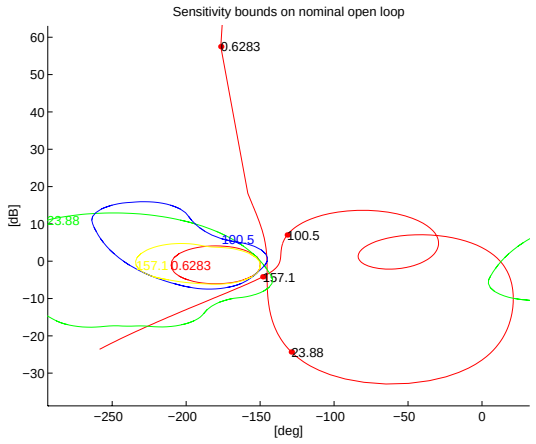

Figure 3: Sensitivity bounds for some frequencies (rad/s) together with the compensated nominal loop of the G_{high} design.

A simulation [6] for the nominal case shows that the biggest torque overshoot is 75% and the biggest impact drop on the load side is only 0.38 rad.

3.1 Linear Design for the Plant with Backlash

However, with backlash, the controller G_{high} causes large limit cycles for an operating point with the load torque $T_d = 0$, while a simulation with the PI controller exhibits no limit cycles, see figure 7. The high performance of the G_{high} controller is hence not practically useful if the plant includes backlash. The effect of backlash needs to be included in the design. Therefore an additional controller, G_{low} is designed, which avoids the limit cycle, and has better performance than the PI-controller.

Let $N_b(A, T_0, w)$ denote the describing function of the shaft with backlash, equation (3)-(4), where A denotes the input amplitude, and T_0 the operating point, as defined by a constant load torque $T_d = T_0$. See [6]. Replacing equation (2) with $T_s = N_b\theta_d$ the equivalent plant transfer function from motor torque reference to motor speed becomes

$$P_b = \left(\frac{e^{-s\tau_d}}{(1+s\tau_e)}\right)\left(\frac{J_l s^2 + c_l s + N_b}{d_b(s)}\right) \qquad (10)$$

where

$$d_b(s) = J_m J_l s^3 + (J_l c_m + J_m c_l)s^2 +$$

$$+((J_l + J_m)N_b + c_m c_l)s + (c_m + c_l)N_b$$

Consider N_b as an uncertain complex parameter, dependent on k_s, c_s, A and, T_0. By letting $A \in (0, \infty)$ and $T_0 \in [0, \infty)$, P_b defines larger templates than the the linear plant.

An analysis using the exact backlash model [5] shows that the system controlled by G_{high} would exhibit no limit cycles when T_0 becomes large. In figure 7 this is verified; the limit cycle does not start until the load torque T_d goes to zero. Hence, following [7], limit cycle avoidance can be analyzed as a stabilization problem for the uncertain plant P_b, by the following additional specification: 5) DF stability specification: $|S_b(j\omega)| < 12$ dB, where S_b denotes the sensitivity function with the plant equal to P_b.

It turns out that the DF stability specification is fulfilled when the open loop is $G_{\mathrm{PI}}P_b$, but not when it is $G_{\mathrm{high}}P_b$. A new controller, $G_{\mathrm{low}} \stackrel{\mathrm{def}}{=} G(g_{\mathrm{low}})$ with $g_{\mathrm{low}} = \{k_p = 80; T_i = 0.2; \omega_1 = 100; \zeta_1 = 0.15; \omega_2 = 100\ \zeta_2 = 0.35; \omega_3 = 45; \zeta_3 = 0.45; \omega_4 = 35; \zeta_4 = 0.5\}$ was designed to fulfill also the DF stability specification. This controller has $k_p/T_i = 80/0.09 \approx 890$.

A Nichols plots of the open loop $G_{\mathrm{low}}P_b$ for a representative set of plant cases is shown in 4 See [6] for Nichols plots of $G_{\mathrm{PI}}P_b$ and $G_{\mathrm{high}}P_b$. In figure 7 closed

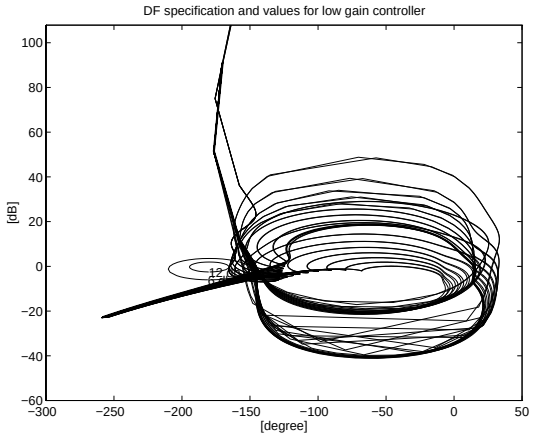

Figure 4: Nichols plots of the open loop $G_{low}P_b$ for a representative set of plants. All cases are stable, fulfilling $|S_b(w)| < 12$ dB.

loop simulations of the plant with backlash are shown when using the three controllers G_{PI}, G_{high}, and G_{low}, respectively. Exactly as indicated by the Describing Function analysis, the simulation shows that the high gain controller gives rise to limit cycles, whereas the two other controllers yield stable closed loop systems.

4 Design of Non-linear Controller

In this section the two controllers G_{high} and G_{low} are combined into one controller $G_{switched}$, by soft switching. The performance of $G_{switched}$ will be shown to be almost as good as the performance of G_{high}, without causing limit cycles.

One novel idea in this work is that the switching is based on the *controller output* i.e. the motor torque

reference, and not, as in [1, 2] on the current backlash angle which is usually difficult to measure or estimate. A high motor torque keeps the backlash gap closed, and then G_{high} can be used. For low or zero motor torque, the backlash gap may be open and then G_{low} is used. For intermediate torque levels an interpolation or soft switching is utilized.

The idea to switch or gain schedule between two control strategies is not new. The novel idea here is to add correction terms to the controller states, that reduce the transient response of the switching.

4.1 DF Stability of the Switched Controller

It is proposed that all parameters of the linear controller are gain scheduled with respect to the scheduling parameter $v \in [0, 1]$. Assume for the moment that v is constant. Then a switched scheduled controller follows naturally as

$$G_{switched}(v) \stackrel{\text{def}}{=} G_(g_{low} + v(g_{high} - g_{low})) \qquad (11)$$

For each constant v, one may calculate the minimum value of the operating point T_0, for which the describing function stability test holds. See figure 5. To check the

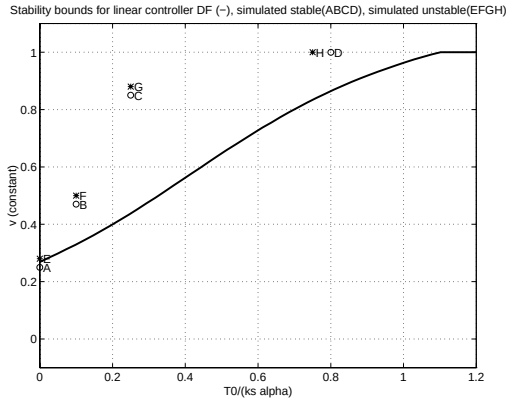

Figure 5: Stability test for different constant values of v in equation (11) as a function of $T_0/(k_s\alpha)$. Above the solid line, the describing functions predicts limit cycles. The points A-D show no limit cycles in simulation, as opposed to the points E-H which do.

result, the closed loop system for some pairs (T_0, v) were simulated, indicating that the describing function limit is conservative.

Based on figure 5, a function was chosen:

$$v(T) = \begin{cases} 0 & |T| \le T_{\min} \\ \frac{|T| - T_{\min}}{T_{\max} - T_{\min}} & T_{\min} < |T| < T_{\max} \\ 1 & T_{\max} \le |T| \end{cases} \qquad (12)$$

where $T_{\min}$ and $T_{\max}$ are the tuning parameters with $0 < T_{\min} < T_{\max}$. Choosing $T_{min} = 0$, and $T_{max} = 165$ Nm $= k_s\alpha$ we are well below the simulated limit cycles in figure 5.

4.2 Controller Design

In this section the final non-linear controller is designed. First, not knowing the operating point, the switching parameter v is instead based on the controller output T_r, i.e. let $v = v(T_r)$. Then the pseudo linear controller $G_{switched}$ from (11) needs to be modified to cope with a time varying v.

The backlash gap can be open only if the shaft torque is zero [6]. Ideally the gain scheduling should be based on the shaft torque. Here only the motor speed ω_m is measured. If the motor inertia is small relative to the load inertia, it holds that the motor torque and shaft torque are approximately equal, and the motor torque reference, i.e. the control input, can be used as scheduling parameter. If the motor inertia is large with respect to the load inertia a linear controller is almost as good as a switched one [6].

The controller in chosen to be implemented in real factored form, as in figure 6. For each block the effects of the scheduling is compensated and analyzed separately.

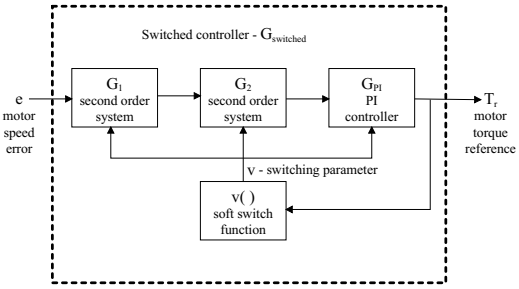

Figure 6: Block diagram of the switched controller $G_{switched}$.

4.2.1 Softly Switched Second Order Filter:

Consider a second order transfer function. Its low frequency gain can be chosen to one without loss of generality.

$$G(s, \omega_1(v), \zeta_1(v), \omega_2(v), \zeta_2(v)) = \frac{s^2/\omega_1^2 + 2\zeta_1/\omega_1 + 1}{s^2/\omega_2^2 + 2\zeta_2/\omega_2 + 1} \qquad (13)$$

where $v = v(T_r)$ is the now time varying switching parameter, and T_r is the motor torque reference. (13) is implemented in state space form as

$$\begin{bmatrix} \dot{x_1} \\ x_2 \end{bmatrix} = A(v) \begin{bmatrix} x_1 \\ x_2 \end{bmatrix} + B(v)u + \begin{bmatrix} x_{1c}(x, \dot{v}) \\ x_{2c}(x, \dot{v}) \end{bmatrix}$$

$$A(v) = \begin{bmatrix} -\zeta_2(v)\omega_2(v) & 1 \\ -\omega_2^2(v) & 0 \end{bmatrix}$$

$$B(v) = \begin{bmatrix} \zeta_1(v)\omega_1(v) - \zeta_2(v)\omega_2(v) \\ \omega_1^2(v) - \omega_2^2(v) \end{bmatrix}$$

$$C = \begin{bmatrix} 1 & 0 \end{bmatrix}$$

$$D(v) = (\omega_2(v)/\omega_1(v))^2$$
$$y = Cx + D(v)u \tag{14}$$

where u is the input, y is the output, and

$$x_c(x, \dot{v}) = \begin{bmatrix} x_{1c}(x, \dot{v}) \\ x_{2c}(x, \dot{v}) \end{bmatrix}$$

is introduced as a correction term which must fulfill $x_c(x, \dot{v} = 0) = 0$. For v constant, i.e. for $\dot{v} = 0$, the system (14) behaves as a second order LTI transfer function (13).

Preferably the time variations of v should not affect the dynamics of the system (14). Computing the time derivative of the output y, noting that $\dot{C} = 0$ we obtain

$$\dot{y} = CAx + CBU + D\dot{u} + (Cx_c + \dot{D}u) \tag{15}$$

In order not to let (15) depend directly on $\dot{v}$ it must hold that

$$Cx_c = -\dot{D}u \tag{16}$$

from which it follows that

$$\dot{y} = CAx + CBU + D\dot{u} \tag{17}$$

The time derivative of (17) is

$$\ddot{y} = CA(Ax + Bu) + CB\dot{u} +$$
$$+D\ddot{u} + (CAx_c + C\dot{A}x + C\dot{B}u + \dot{D}\dot{u}) \tag{18}$$

To avoid that $\ddot{y}$ depends on $\dot{v}$ it must hold that

$$CAx_c = -C\dot{A}x - C\dot{B}u - \dot{D}\dot{u} \tag{19}$$

From equations (16) and (19) $x_c(x, \dot{v})$ can be calculated to

$$x_c(x, \dot{v}) = \begin{bmatrix} C \\ CA(v) \end{bmatrix}^{-1} \begin{bmatrix} -D_v u \\ -CA_v x - CB_v u - D_u \dot{u} \end{bmatrix} \dot{v} \tag{20}$$

where we used the notation $A_v = \partial A/\partial v$. Since this second order system is observable by construction, equation (20) can always be solved, uniquely defining the state compensation x_c.

By using the correction term x_c, the switching can now be very fast, without causing unwanted transients in the controller output. A similar non-linear state equation can be obtained for the PI-controller in figure 6, into which the overall low frequency gain can be included.

5 Experiments on an Industrial Drive System

Simulations with the switched controller are found in figure 7 and in [6]. The switched controller was also implemented and tested in discretized form on a modern drive system of PWM type, consisting of a 1.5 MW

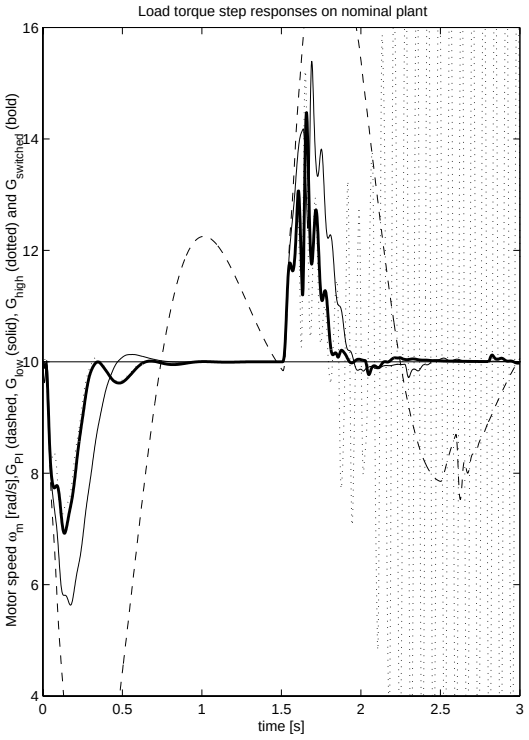

Figure 7: Closed loop simulations of load step responses for the four designed controllers G_{PI} (dashed), G_{high} (dotted), G_{low} (solid) and $G_{switched}$ (solid bold) controlling the nominal plant with backlash. It can be seen that $G_{switched}$ combines the best properties of G_{low} and G_{high}.

synchronous motor, delivering a maximum of 20 kNm, connected to a load torque producing DC motor of 1 MW, via a flexible coupling filled with oil. From an open loop motor torque step response, it was estimated that the resonance frequency was 8.0 Hz. The ratio between the motor and load moments of inertia were guessed to $J_l/J_m \approx 2$, by inspection of the rotor sizes.

First a low gain controller $G_l = G(g_l)$ was manually tuned to be a PI controller, in the form of (9) with $g_l = \{k_p = 5; T_i = 0.2; \omega_1 = 2\pi 7; \zeta_1 = 0.5; \omega_2 = 2\pi 7; \zeta_2 = 0.5\}$.

The tuning was carried out as follows: With $T_i = \infty$, k_p was increased to the closed loop stability limit, and then detuned by a factor 2. T_i was then decreased until an overshoot appeared in the speed response to a load torque step and then T_i was slightly increased.

Then a high gain controller $G_h = G(g_h)$ was tuned, using a non-zero load torque, with $g_l = \{k_p = 15; T_i = 0.2; \omega_1 = 2\pi 7; \zeta_1 = 0.1; \omega_2 = 2\pi \cdot 5.5; \zeta_2 = 0.35\}$ to include an asymmetric notch filter. The low high frequency gain of the notch filter made it possible to increase the gain k_p to 15. Then a switching controller G_s with T_{min}=200 Nm and T_{max}=500 Nm, was tested.

In figures 8-9 measurements of load torque step responses are shown for all three controllers G_{l}, G_{h} and G_{s}. The results are strikingly similar to the simulations in this paper and in [6], and show that the proposed non-linear control strategy might work in practice.

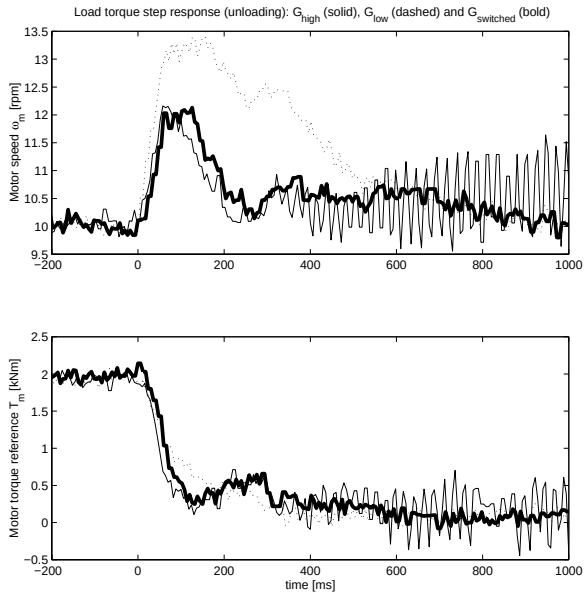

Figure 8: Measurements of a load torque step response on the industrial sized two-mass drive system, for the three designs. Note the large impact drop area with the low gain linear controller G_{l} (dotted), and the limit cycle oscillations with the high gain controller G_{h} (solid), after the load torque is set to zero for $t > 0$. It can be clearly seen that the non-linear controller G_{s} (bold) combines high performance with stability, i.e. low impact drop area, and no limit cycles.

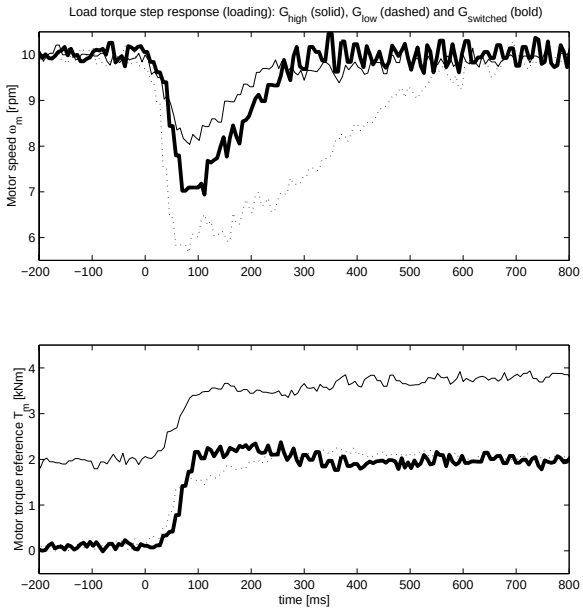

Figure 9: Measurements of a load torque step response on the industrial sized two-mass drive system, for the three designs. Note the large impact drop area for the low gain linear controller G_{l} (dotted), and the high performance of the high gain controller G_{high} (solid). The switched controller G_{s} (bold) has almost the same high performance. Note that the experiment with the high gain controller is performed with a non-zero load torque. Otherwise the high gain controller would have caused serious limit cycle oscillations.

6 Conclusions

The control design in this paper follows the paradigm "weak action in the backlash gap". This paradigm has been more successful than the opposing "strong action in the backlash gap", see [6].

The design method is easily extended to multi-mass systems, with several backlashes, and can simultaneously be modified to cope with non-linear actuator characteristics.

Further research in this area also include proofs of stability for the non-linear and linear control strategies, e.g. with piece-wise quadratic Lyapunov functions [4] which are currently being prepared for publication.

References

[1] R. Boneh and O. Yaniv. Control of an elastic two-mass system with large backlash. *J. of Dynamic Systems, Measurement and Control*, 1998.

[2] B. Friedland. Feedback control of systems with parasitic effects. In *Proc. of ACC-97*, Albuquerque, USA, 1997. American Automatic Control Council.

[3] Isaac M. Horowitz. *Quantitative Feedback Design Theory (QFT)*. QFT Publications, Boulder Co, 1992.

[4] M. Johansson. *Piecewise Linear Control Systems*. PhD thesis, Dept. of Automatic Control, Lund University, Sweden, 1999.

[5] M. Nordin, J. Galic, and P.O. Gutman. New models for backlash and gear play. *Int J. of Adaptive Control and Signal Processing*, 1:9–63, 1997.

[6] Mattias Nordin. *Nonlinear backlash compensation for speed controlled elastic systems*. Phd thesis, TRITA-MAT-00-OS3, Division of Optimization and Systems Theory, Royal Institute of Technology, 10044 Stockholm, Sweden, 2000.

[7] S. Oldak, C. Baril, and P. O. Gutman. Quantative design of a class of nonlinear systems with parameter uncertainty. *Int J. of Robust and Nonlinear Control*, 4:101–117, 1994.